

# Echocardiography in Saanen-goats: Normal findings, reference intervals in awake goats, and the effect of general anesthesia\*

K. Steininger<sup>2</sup>, A.-S. J. Berli<sup>1</sup>, R. Jud<sup>1</sup>, C. C. Schwarzwald<sup>1</sup>

<sup>1</sup>Equine Department and <sup>2</sup>Farm Animal Department, University of Zurich

\*Herrn Prof. Dr. Ueli Braun zu seinem 60. Geburtstag gewidmet

## Summary

Echocardiographic assessment of cardiac structures, dimensions, and mechanical function in goats is poorly documented. The goal of this study was to describe normal findings, establish normal values for two-dimensional (2DE) and M-mode (MME) echocardiography, and investigate the influence of general anaesthesia.

Standardized 2DE and MME recordings were obtained on 22 healthy female Saanen goats ( $3.7 \pm 1.1$  years [mean  $\pm$  SD],  $60.2 \pm 10.6$  kg) awake (standing) and during isoflurane anesthesia (sternal recumbency). Cardiac dimensions and function were assessed and compared between treatments (awake vs. anaesthetized). Color Doppler imaging and saline contrast studies served to assess abnormal blood flow patterns. Post mortem examination was performed in a subset of 12 goats. Transthoracic echocardiography was feasible in all goats.

Indices of LV systolic function proved to be significantly increased during general anesthesia. The membranous and occasionally echolucent appearance of the oval fossa suggested abnormal interatrial communication in 9 goats. Color Doppler imaging and saline contrast studies proved to be inaccurate to detect interatrial shunting of blood. Post mortem examination confirmed small persistent foramen ovale in only 3 out of 7 goats, in which it had been suspected on echocardiography.

Keywords: goat, echocardiography, anesthesia, reference intervals, persistent foramen ovale

## Echokardiographie bei Saanenziegen: Normalbefunde, Referenzwerte bei wachen Ziegen und der Einfluss einer Allgemeinanästhesie

Die echokardiographische Beurteilung von Struktur, Grösse und mechanischer Funktion des Herzens wurde bisher bei Ziegen kaum untersucht. Das Ziel dieser Studie war es, Normalbefunde zu beschreiben, Referenzwerte für 2-dimensionale (2DE) und M-Mode echokardiographische (MME) Untersuchungen festzulegen und den Einfluss einer Allgemeinanästhesie zu prüfen. Standardisierte echokardiographische Messungen in 2DE und MME wurden an 22 gesunden weiblichen Saanenziegen ( $3.7 \pm 1.1$  Jahre [Mittelwert  $\pm$  SD],  $60.2 \pm 10.6$  kg) in wachem Zustand (stehend) und unter Allgemeinanästhesie mit Isofluran (in Brustlage) durchgeführt. Grösse und Funktion des Herzens wurden beurteilt und zwischen den beiden Untersuchungen (wach bzw. anästhesiert) verglichen. Farb-Doppler Ultraschall und Kontraststudien mit Kochsalzlösung dienten der Beurteilung von abnormalen Blutfluss-Mustern. Bei einer Untergruppe von 12 Ziegen wurde eine postmortale Untersuchung durchgeführt.

Die transthorakale echokardiographische Untersuchung war bei allen Ziegen durchführbar. Die Messwerte, die die linksventrikuläre systolische Funktion beschreiben, erwiesen sich während der Allgemeinanästhesie als signifikant erhöht. Die membranöse und gelegentlich anechogene Erscheinung der Fossa ovalis liess bei 9 Ziegen eine abnormale Verbindung zwischen den Vorhöfen vermuten. Die Farb-Doppler Ultrasonographie und die NaCl-Kontraststudien erwiesen sich als ungenaue Methoden, um einen Shunt zwischen den Vorhöfen zu erkennen. Bei der postmortalen Untersuchung konnte ein kleines persistierendes Foramen ovale nur bei 3 von 7 Ziegen, bei welchen es aufgrund der Echokardiographie vermutet worden war, bestätigt werden.

Schlüsselwörter: Ziege, Echokardiographie, Anästhesie, Referenzwerte, persistierendes Foramen ovale

## Introduction

Transthoracic echocardiography is a non-invasive diagnostic tool for assessment of cardiac structures, chamber dimensions, and myocardial function. Two dimensional echocardiography (2DE), M-mode echocardiography (MME), and Doppler echocardiography are routinely used in the diagnostic workup of heart disease in humans and animals (Feigenbaum et al., 2005; Boon, 2011). State-of-the-art echocardiography equipment with digital raw data storage allows high-quality imaging of hearts in a wide range of species at different sizes. Normal findings and reference intervals for echocardiographic measurements have been reported for a variety of species (Boon, 2011). As of February 2011, a PubMed search using the term «echocardiography» in combination with the terms «cow», «sheep», and «goat», respectively, returned 211, 464, and 34 hits. However, the vast majority of these publications relate to the use of these animal species as research models of human disease or as donors for heterologous tissue grafts. Others describe single cases or small case series of ruminants with cardiac disease. Only few reports focus on echocardiography in healthy ruminants. Pipers et al. (1978), Braun and Schweizer (2001), Braun et al. (2001), Hallowell et al. (2007), and Buczinski (2009) described the use of echocardiography in adult cattle and reported on normal values for 2DE and MME measurements. Three publications exist on echocardiography in healthy calves (Amory and Lekeux, 1991; Amory et al., 1991; Amory et al., 1992) and one report concerns the use of M-mode echocardiography in sheep (Moses and Ross, 1987). Finally, Olsson et al. (2001) studied changes in cardiac size and function by echocardiography in 8 Swedish domestic goats during pregnancy, lactation, and the dry period, and Acorda et al. (2005) described the ultrasonographic features of the heart in Philippine native goats. However, to the authors' knowledge there are no other reports concerning echocardiographic assessment of cardiac dimensions and mechanical function in the healthy adult goat. Furthermore, there are no studies investigating the influence of general anesthesia on echocardiographic variables in this species.

The aim of this study was therefore to describe normal findings, establish normal values for echocardiographic variables of cardiac dimensions and cardiac mechanical function in awake goats, and to investigate the influence of general anaesthesia on echocardiographic variables.

## Animals, Material and Methods

### Animals

22 female Saanen goats aged  $3.7 \pm 1.1$  years [mean  $\pm$  SD] and with a body weight (BWT) of  $60.2 \pm 10.6$  kg were studied prospectively. All goats were considered healthy based upon physical examination, cardiac auscultation, and routine echocardiographic examination. The goats

were non-pregnant and they were at the end of lactation. None of the goats received medications during the 2 weeks preceding entry into the study. The goats were acclimatized to the hospital for one week before entry into the study. They were housed indoors, kept on straw, and had free access to water and hay. Animal experiments were carried out in accordance with the Swiss law on animal protection and were approved by the district veterinary office of the Canton Zurich, Switzerland.

### Study design

All goats underwent a complete echocardiographic examination while standing in a quiet room, unsedated and restrained by an experienced handler. The goats underwent a second echocardiographic examination within  $7.41 \pm 3.45$  days of the first examination. This second examination was performed immediately following a computed tomography scan conducted within the scope of other investigations (Irmer, 2010; Makara, 2010; Ohlert et al., 2010), with the goats in general anesthesia and positioned in sternal recumbency. The mean time from induction of anesthesia to the start of the echocardiographic examination was 68 (52–103) min [mean (range)].

### General anesthesia

The animals were fasted for 24 h and deprived of water for 2 h prior to anesthesia. All animals were premedicated with  $0.1 \text{ mg kg}^{-1}$  xylazine (Rompun 2%, Provect, Lys-sach, Switzerland), diluted in 20 mL of saline (NaCl 0.9%, Braun Medical, Sempach, Switzerland), given intravenously (IV) over 5 min. Anesthesia was induced with either  $3 \text{ mg kg}^{-1}$  racemic ketamine (Narketan 10%, Vetoquinol, Ittigen, Switzerland) or  $1.5 \text{ mg kg}^{-1}$  S-ketamine (Keta-S 6%, Dr. Graeub AG, Bern, Switzerland) IV. After induction, the goats were positioned sternally, intubated, and connected to an anesthesia machine. Generally, the goats were allowed to breathe spontaneously throughout the entire duration of anesthesia. Intermittent positive pressure ventilation (tidal volume 10–15 mL  $\text{kg}^{-1}$ , rate 10–15 breaths  $\text{minute}^{-1}$ ) was only applied when arterial blood gas analysis revealed a  $\text{P}_a\text{CO}_2 > 50$  mmHg. Anesthesia was maintained with isoflurane (IsoFlo®, Abbott, Baar, Switzerland) delivered in oxygen and air via a semi-closed circle absorption system. The vaporizer was set to maintain an end-tidal concentration of 1.1% isoflurane. Lactated Ringer's solution (Ringer-Laktat, Fresenius Kabi, Stans, Switzerland) was administered IV at a dose rate of  $10 \text{ mL kg}^{-1} \text{ h}^{-1}$ . For further details concerning general anesthesia, instrumentation, and monitoring, the reader shall be referred to a previous publication (Jud et al., 2010).

### Echocardiography

Transthoracic echocardiography was performed using a high-end digital echocardiograph (GE Vivid 7 Dimen-

sion, BTO6, GE Medical Systems, Glattbrugg, Switzerland) with a M4S phased-array transducer at a frequency of 1.9/4.0 MHz (octave harmonics) and a frame rate of 85.3 frames/sec. A single-lead electrocardiogram was recorded simultaneously for correct timing of measurements within the cardiac cycle. All echocardiographic recordings were performed by the same operator (CCS) according to a standard protocol and stored as cine-loops in digital raw data format. Data analyses were performed offline, blinded, and in random order by a second operator (KS) using a dedicated software package (EchoPAC Software Version 6.1.2, GE Medical Systems). Whenever the recorded echo loops did not allow unequivocal identification of anatomical landmarks (e.g., because of imaging artefacts or poor image quality) or adequate timing of measurements (e.g., because of motion artefacts on the surface ECG), measurements were not performed. Three representative, non-consecutive cardiac cycles were analyzed for each variable and the average of the three measurements was used for data analyses and statistics.

Two-dimensional, M-mode, and color Doppler echocardiography were performed in standard right parasternal long-axis and short-axis imaging planes to assess cardiac structures, large vessels, valvular competence, integrity of atrial and ventricular septum, chamber dimensions, and left ventricular (LV) and left atrial (LA) mechanical function (Lang et al., 2006; Schwarzwald et al., 2007; Schefer et al., 2010; Boon, 2011).

The long-axis planes included a right ventricular outflow tract (RVOT) view (Fig. 1A), a left ventricular outflow tract (LVOT) view (Fig. 1B), a four-chamber view optimized to obtain an image of the entire LA at its maximal dimensions (Fig. 1C), and a four-chamber view optimized to obtain an image of the LV at its maximal dimensions (Fig. 1D). The short-axis planes included a cross-sectional view of the LA at the level of the aortic valve (Fig. 2A) and a cross-sectional view of the LV at the level of the chordae tendineae (Fig. 2B).

Color Doppler imaging of intra- and inter-atrial blood flow and saline contrast studies (by rapidly injecting a

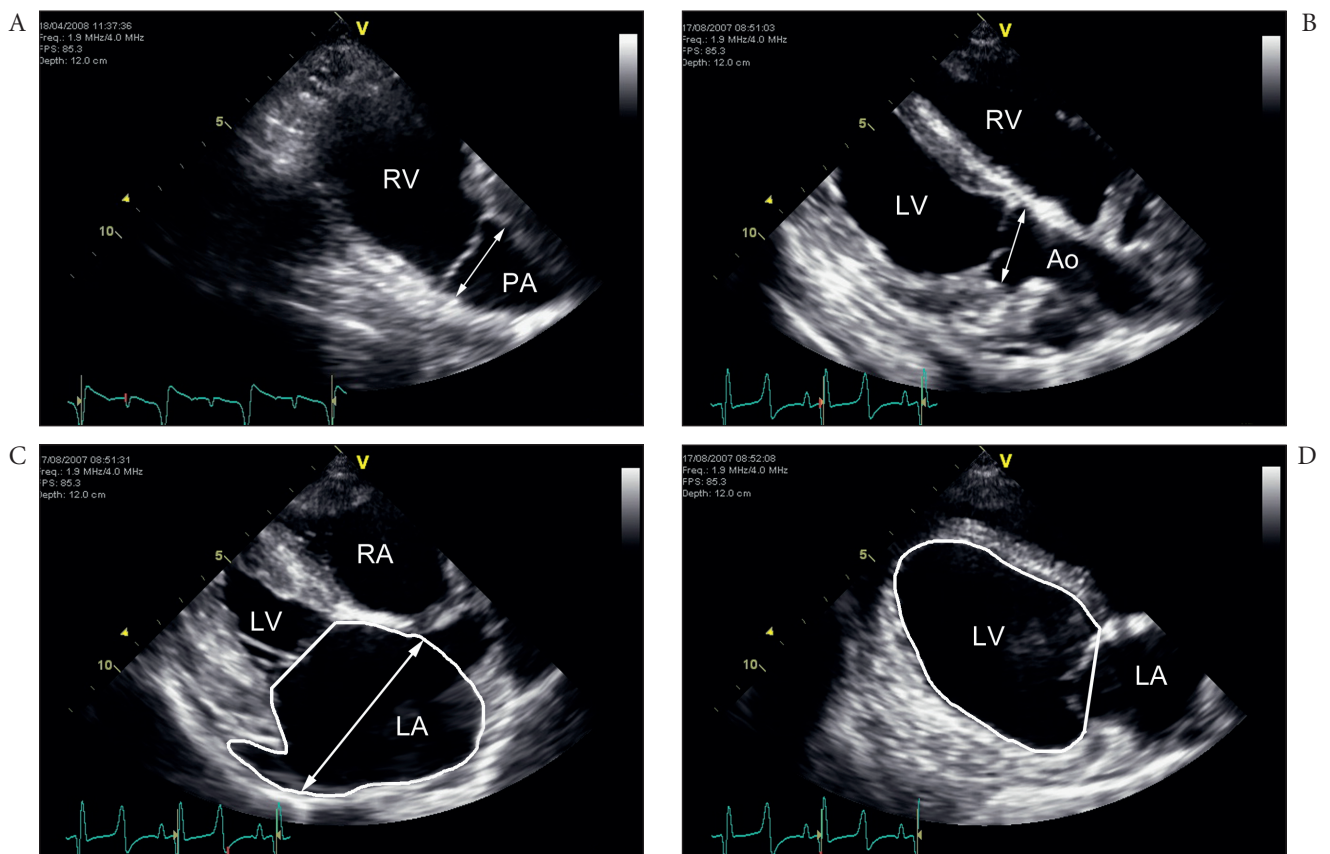


**Figure 1:** Two-dimensional echocardiograms obtained from right parasternal long-axis views. An ECG is recorded simultaneously for timing. A, Right-ventricular outflow tract view at end-diastole. The pulmonary artery diameter (PAD) is marked with a double arrow. B, Left-ventricular outflow tract view at end-diastole. The aortic diameter (AoD) is marked with a double arrow. C, Four-chamber view at end-systole, optimized to obtain an image of the entire left atrium (LA) at its maximal dimensions. The LA maximal diameter (LAD<sub>max</sub>; double arrow) and the LA maximal area (LAA<sub>max</sub>; tracing) were measured as shown. D, Four-chamber view at end-diastole, optimized to obtain an image of the left ventricle (LV) at its maximal dimensions. The LV internal area (LVIAD) was traced as shown. Ao, Aorta; LA, left atrium; LV, left ventricle; PA, pulmonary artery; RA, right atrium; RV, right ventricle.

## 556 Originalarbeiten

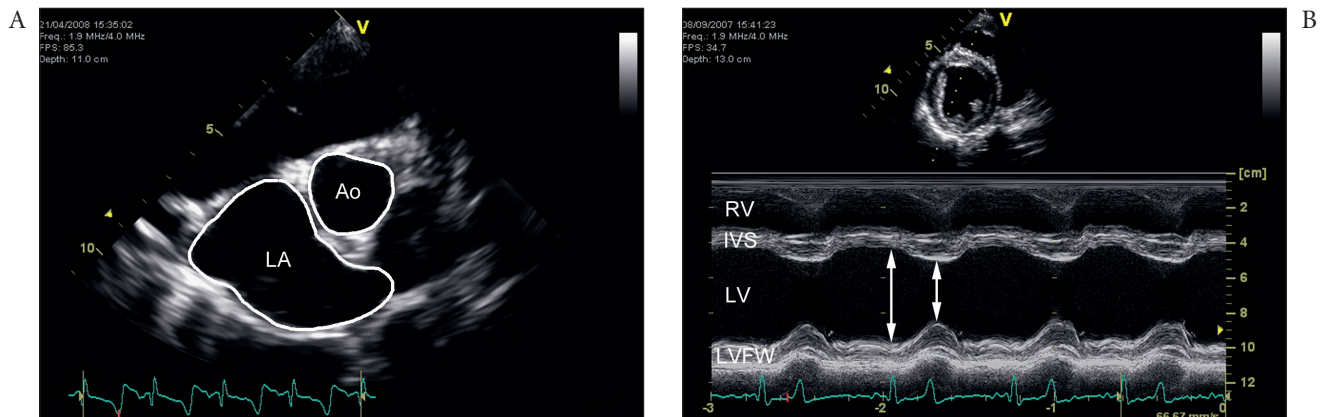


**Figure 2:** Echocardiograms obtained from right parasternal short-axis views. An ECG is recorded simultaneously for timing. **A,** End-systolic 2DE recording of the left atrium (LA) at the level of the aortic valve (Ao). The LA maximal area in short axis ( $LA_{sxA}$ ) and the area of the aortic root ( $Ao_{sxA}$ ) were traced as indicated. **B,** M-mode echocardiogram of the left ventricle (LV) obtained in a right parasternal short-axis view at the level of the chordae tendineae. The LV internal diameter at end-diastole ( $LVID_d$ ; long double arrow) and the LV internal diameter at peak systole ( $LVID_s$ ; short double arrow) were measured as indicated. Ao, Aorta; IVS, interventricular septum; LA, left atrium; LV, left ventricle; LVFW, left-ventricular free wall; RV, right ventricle.

bolus of 20 mL of agitated normal saline through a jugular venous catheter) were performed to screen for patent foramen ovale (PFO) or atrial septal defects (ASD) in all goats, in which the oval fossa appeared particularly large and thin, was echolucent, or had a marked flailing or billowing appearance. When performed during general anesthesia, positive airway pressure was applied for the duration of the saline contrast study to increase the likelihood of right-to-left shunting and to facilitate the diagnosis of a defect by saline contrast study.

The end-diastolic pulmonary artery diameter (PAD) was measured in the RVOT view as the distance across the sinus, parallel to the line that connects the pulmonary artery annulus (Fig. 1A). The end-diastolic aortic diameter (AoD) was measured in the LVOT view as the distance across the sinus of Valsalva, parallel to the line that connects the aortic annulus (Fig. 1B). The AoD/PAD ratio was calculated. The aortic annular diameter (AAD) was measured in the LVOT view as the inner distance between the opened aortic valve leaflets during peak systole.

Size and mechanical function of the left atrium (LA) were assessed as previously described for horses (Schwarzwald et al., 2007). The LA maximal diameter ( $LAD_{max}$ ) and the LA maximal area ( $LAA_{max}$ ), respectively, were measured in the four-chamber view optimized for the LA, one frame before opening of the mitral valve (Fig. 1C).  $LAD_{max}$  was measured as the widest distance from the septal wall to the pericardial lining of the free wall, parallel to the mitral valve annulus. For area measurement of the LA, the caliper was traced along the inner edge of the septal wall and atrial roof and the outer edge (pericardial lining) of the free wall. The confluences of the pulmonary veins were excluded and the ventral border was represented by the plane of the mitral annulus. LA area was also measured at the onset of atrial contraction (i.e., at the onset of the electrocardiographic P wave;  $LAA_a$ ) and at its minimum dimensions

(i.e., at the time of closure of the mitral valve;  $LAA_{min}$ ). Left atrial passive and active emptying was characterized by use of calculated ejection-phase indices, including passive [Passive FAC =  $(LAA_{max} - LAA_a) / LAA_{max} \times 100$ ], active [Active FAC =  $(LAA_a - LAA_{min}) / LAA_a \times 100$ ], and total [Total FAC =  $(LAA_{max} - LAA_{min}) / LAA_{max} \times 100$ ] LA fractional area change. Active emptying was further assessed by calculating the ratio of active to total area change [Active:total AC =  $(LAA_a - LAA_{min}) / (LAA_{max} - LAA_{min})$ ].

The LA maximal area in short-axis ( $LA_{sxA}$ ) was measured in a right parasternal short-axis view at end systole (i.e., 1 frame after closure of the aortic valve) by tracing the inner edge, and indexed to the area of the aortic root ( $Ao_{sxA}$ ) traced in the same imaging plane (Fig. 2A). Functional indices were not determined in the short-axis plane.

Standard LV measurements were performed on M-Mode recordings in a right parasternal short-axis view at the chordal level (Schefer et al., 2010; Boon, 2011). The following variables were measured (Fig. 2B): Interventricular septal thickness ( $IVS_d$ ,  $IVS_s$ ), LV internal diameter ( $LVID_d$ ,  $LVID_s$ ), and left ventricular free wall thickness ( $LVPW_d$ ,  $LVPW_s$ ) using the “trailing-inner-inner-leading edge” method. End-diastolic-measurements (d) were performed at the peak of the electrocardiographic R wave, because the onset of the R wave was not always clearly discernible. Systolic measurements (s) were taken at peak systole, at the time of maximum excursion of IVS and LVFW, respectively. The LV fractional shortening (FS) was calculated as an index of LV systolic function by the following equation:  $FS (\%) = (LVID_d - LVID_s) / LVID_d \times 100$ . The relative wall thickness at end-diastole and at peak systole was calculated as  $RWT_d = (IVS_d + LVPW_d) / LVID_d$  and  $RWT_s = (IVS_s + LVPW_s) / LVID_s$ , respectively. The mean wall thickness at end-diastole and at peak systole was calculated as  $MWT_d = (IVS_d + LVPW_d) / 2$  and  $MWT_s = (IVS_s + LVPW_s) / 2$ , respectively. The  $LAD_{max}/LVID_d$  ratio was calculated. The

instantaneous heart rate (HR) of each measured cycle was derived from the respective RR interval ( $HR = 60000 / RR$  interval).

The internal LV area was measured at end-diastole (LVIA<sub>d</sub>) and peak systole (LVIA<sub>s</sub>) in the right parasternal 4-chamber view optimized for the LV by tracing the endocardial border (Fig. 1D). The LV fractional area change [LV FAC (%) =  $(LVIA_d - LVIA_s) / LVIA_d \times 100$ ] was calculated as an index of LV systolic function. The LAA<sub>max</sub>/LVIA<sub>d</sub> ratio was calculated. LV internal volume at end-diastole (LVIV<sub>d</sub>) and at peak systole (LVIV<sub>s</sub>) were calculated using the single-plane Simpson's method (Lang et al., 2006). The instantaneous HR of each measured cycle was calculated based on the RR interval ( $HR = 60000 / RR$  interval). The ejection fraction [EF =  $(LVIV_d - LVIV_s) / LVIV_d \times 100$ ], the stroke volume [SV =  $LVIV_d - LVIV_s$ ], the stroke volume index [SVI =  $SV / BWT$ ], the cardiac output [CO =  $SV \times HR$ ], and the cardiac index [CI =  $CO / BWT \times 1000$ ] were calculated.

As the study population showed a wide range of BWT, echocardiographic measurements reflecting size of the great vessels and chamber dimensions (i.e., diameters, areas, and volumes) were corrected for differences in BWT according to the principles of allometric scaling (Brown et al., 2003; Cornell et al., 2004). Specifically, the measurements were normalized to a BWT of 60 kg [60] using the following equations: Linear Dimension [60] = Measured

Linear Dimension /  $BWT^{1/3} \times 60^{1/3}$ ; Area [60] = Measured Area /  $BWT^{2/3} \times 60^{2/3}$ ; and Volume [60] = Measured Volume /  $BWT \times 60$ . Furthermore, measurements were indexed to AAD (linear measurements), AAD<sup>2</sup> (area measurements), and AAD<sup>3</sup> (volume measurements), respectively, using the aortic annular diameter as an inherent surrogate of body size.

### Post mortem examination

Twelve goats were available for post mortem examination after humane euthanasia that was performed within the scope of another study. Great vessels, chamber size, myocardial and valvular structures, the integrity of the interventricular septum, and the integrity of the atrial septum, were assessed by gross inspection. The oval fossa was explored by use of a small probe to assess patency of the foramen ovale.

### Data analysis and statistics

Statistical and graphical analyses were performed using standard computer software (Microsoft Office Excel 2003, Microsoft Corporation, Redmond, WA; SigmaStat v3.5, SPSS Inc, Chicago, IL; GraphPad Prism v5.00 for Windows, GraphPad Software, San Diego, CA). Summary statistics, including mean, standard de-

Table 1: Echocardiographic dimensions of aorta and pulmonary artery measured using two-dimensional echocardiography (2DE).

Variable	Units	Awake			Anesthetized			Paired t-Test		
		n	Mean ± SD	5–95% percentile	n	Mean ± SD	5–95% percentile	95% CI for difference of means	p-value	Significant after Bonferroni correction (P < 0.0056)
Aorta and Pulmonary Artery										
PAD	cm	15	2.6 ± 0.3	2.1–3.3	20	2.7 ± 0.3	2.2–3.2	-0.01 to 0.29	0.064	n.s.
PAD [60]	cm	15	2.6 ± 0.3	2.0–3.2	20	2.8 ± 0.3	2.2–3.2	-0.01 to 0.28	0.065	n.s.
AoD	cm	22	3.0 ± 0.4	2.2–3.7	21	3.0 ± 0.4	2.4–4.0	-0.13 to 0.12	0.957	n.s.
AoD [60]	cm	22	3.0 ± 0.4	2.5–3.8	21	3.0 ± 0.4	2.4–4.1	-0.13 to 0.12	0.917	n.s.
AoD/PAD		15	1.2 ± 0.1	1.0–1.4	19	1.1 ± 0.1	1.0–1.4	-0.12 to 0.02	0.134	n.s.
AAD	cm	22	2.5 ± 0.2	2.0–2.9	21	2.4 ± 0.2	2.0–2.9	-0.10 to 0.03	0.250	n.s.
AAD [60]	cm	22	2.5 ± 0.2	2.1–3.0	21	2.5 ± 0.2	2.0–3.0	-0.09 to 0.02	0.240	n.s.
Ao <sub>ss</sub> A	cm <sup>2</sup>	22	5.6 ± 1.2	3.8–8.1	22	5.8 ± 1.2	3.7–8.2	-0.17 to 0.62	0.246	n.s.
Ao <sub>ss</sub> A [60]	cm <sup>2</sup>	22	5.6 ± 1.1	4.1–8.2	22	5.8 ± 1.1	3.8–8.6	-0.19 to 0.64	0.270	n.s.

PAD	Pulmonary artery diameter
PAD [60]	Pulmonary artery diameter (normalized to a body weight of 60 kg)
AoD	Aortic diameter
AoD [60]	Aortic diameter (normalized to a body weight of 60 kg)
AoD/PAD	AoD-to-PAD ratio
AAD	Aortic annular diameter
AAD [60]	Aortic annular diameter (normalized to a body weight of 60 kg)
Ao <sub>ss</sub> A	Aortic area in short-axis view
Ao <sub>ss</sub> A [60]	Aortic area in short-axis view (normalized to a body weight of 60 kg)

## 558 Originalarbeiten

viation, and 5 % and 95 % percentiles, respectively, were calculated to describe normal values in awake goats and in goats under general anesthesia. A paired t-test was used to identify differences between the two treatments (awake vs. anesthetized). Because it had been shown previously that there were no significant differences in cardiovascular function during general anesthesia after induction with two different ketamine formulations (racemic ketamine and S-ketamine, respectively) (Jud et al., 2010), the different induction protocols were not further considered in this study. The level of significance was set at  $p = 0.05$ . The 95 % confidence interval for the difference of means was reported. To correct for multiple comparisons, Bonferroni correction was applied to variables of aortic and pulmonary artery size ( $p = 0.05/9 = 0.0056$ ), variables of LA size and function

( $p = 0.05/13 = 0.0039$ ), and variables of LV size and function ( $p = 0.05/35 = 0.0014$ ).

Finally, sensitivity, specificity, positive predictive value, and negative predictive value for echocardiography to diagnose a PFO were calculated based on the subpopulation of goats in which post mortem examination (gold standard) had been performed.

## Results

Echocardiographic examination was possible in all goats, both awake and under general anesthesia. Assessment of great vessel size, LA size and mechanical function, and LV size and mechanical function was readily achieved using 2DE and MME.

Table 2: Echocardiographic variables of left-atrial dimensions and left-atrial mechanical function using two-dimensional echocardiography (2DE).

Variable	Units	Awake			Anesthetized			Paired t-Test		
		n	Mean ± SD	5–95 % percentile	n	Mean ± SD	5–95 % percentile	95 % CI for difference of means	p-value	Significant after Bonferroni correction (P < 0.0039)
Left atrium – 2DE long-axis view										
LAD <sub>max</sub>	cm	22	5.9 ± 0.6	4.8–7.1	22	6.3 ± 0.7	5.2–7.5	0.12 to 0.69	0.008	n.s.
LAD <sub>max</sub> [60]	cm	22	5.9 ± 0.7	4.9–7.2	22	6.3 ± 0.7	5.2–7.5	0.11 to 0.69	0.009	n.s.
LAD <sub>max</sub> /AAD		22	2.39 ± 0.25	1.86–2.88	21	2.58 ± 0.21	2.25–2.97	0.06 to 0.32	0.007	n.s.
LAA <sub>max</sub>	cm <sup>2</sup>	22	21.8 ± 3.8	13.9–28.6	22	23.9 ± 4.2	16.4–33.6	0.39 to 3.79	0.018	n.s.
LAA <sub>max</sub> [60]	cm <sup>2</sup>	22	22.0 ± 4.1	15.9–29.8	22	24.0 ± 4.1	18.2–34.2	0.35 to 3.73	0.020	n.s.
LAA <sub>max</sub> /AAD <sup>2</sup>		22	3.61 ± 0.66	2.29–4.78	21	4.04 ± 0.76	3.06–5.73	0.10 to 0.75	0.014	n.s.
Active FAC	%	22	24.4 ± 9.8	4.2–38.0	22	19.6 ± 8.4	3.8–32.7	-10.62 to 1.00	0.100	n.s.
Passive FAC	%	22	29.5 ± 7.6	18.2–45.9	22	32.0 ± 5.5	22.7–45.9	-1.80 to 6.71	0.243	n.s.
Total FAC	%	22	47.4 ± 7.4	31.9–58.5	22	45.6 ± 6.3	34.2–56.4	-6.09 to 2.51	0.397	n.s.
Active:total AC		22	0.38 ± 0.14	0.06–0.56	22	0.29 ± 0.11	0.07–0.44	-0.16 to -0.01	0.034	n.s.
Left atrium – 2DE short-axis view										
LA <sub>ssA</sub>	cm <sup>2</sup>	22	20.6 ± 3.8	13.1–28.3	22	22.5 ± 3.3	15.1–27.5	0.66 to 3.61	0.007	n.s.
LA <sub>ssA</sub> [60]	cm <sup>2</sup>	22	20.6 ± 4.3	14.0–29.6	22	22.6 ± 3.2	16.6–29.7	0.64 to 3.44	0.006	n.s.
LA <sub>ssA</sub> /Ao <sub>ssA</sub>		22	3.7 ± 0.8	2.7–5.7	22	4.0 ± 0.9	2.8–6.8	-0.17 to 0.64	0.237	n.s.

LAD <sub>max</sub>	Maximal left atrial diameter
LAD <sub>max</sub> [60]	Maximal left atrial diameter (normalized to a body weight of 60 kg)
LAD <sub>max</sub> /AAD	Maximal left atrial diameter indexed to aortic annular diameter
LAA <sub>max</sub>	Maximal left atrial area
LAA <sub>max</sub> [60]	Maximal left atrial area (normalized to a body weight of 60 kg)
LAA <sub>max</sub> /AAD <sup>2</sup>	Maximal left atrial area indexed to the square of aortic annular diameter
Active FAC	Active left-atrial fractional area change
Passive FAC	Passive left-atrial fractional area change
Total FAC	Total left-atrial fractional area change
Active:total AC	Ratio of active-to-total left-atrial area change
LA <sub>ssA</sub>	Left atrial area measured in short-axis view
LA <sub>ssA</sub> [60]	Left atrial area measured in short-axis view (normalized to a body weight of 60 kg)
LA <sub>ssA</sub> /Ao <sub>ssA</sub>	Left atrial area indexed to aortic area measured in short-axis view

The results of the echocardiographic measurements and derived indices as well as the differences between treatments (i.e., awake vs. anesthetized) are summarized in Tables 1 to 3. Heart rate was significantly lower during general anesthesia. Great vessel size was not significantly influenced by general anesthesia as assessed by 2DE (Tab. 1). Individual comparisons of measurements between treatments revealed that a variety of indices of LA and LV size and function were significantly altered during general anesthesia (Tab. 2 and 3). However, after correcting for multiple comparisons within each group of variables (i.e., indices of great vessel size, indices of LA size and function, and indices of LV size and function), only the indices of peak systolic wall thickness (LVFW<sub>s</sub>, MWT, RWT) and the ejection-phase indices of LV systolic function (FS, FAC, EF) proved to be significantly increased by general anesthesia.

The oval fossa was visible as a thin, membranous, occasionally echolucent structure within the interatrial septum (Fig. 3A). It could be clearly identified on 2DE in

21/22 goats in at least one imaging plane (i.e., long-axis view or short-axis view of the LA) and measured between 0.9 and 2.5 (mean 1.5) cm in diameter. In 3 goats, this membrane was billowing to the left, in another 3 goats it was billowing to the right, and in 2 goats it had a flailing appearance. Color Doppler flow mapping atrial blood flow was performed in 10 goats awake and in 18 goats under general anesthesia. It revealed distinct systolic flow in the right atrium, adjacent to the oval fossa, in all goats examined. In 9 goats, a systolic color-coded flow signal also appeared in the left atrium and seemed to cross the interatrial septum in the region of the oval fossa, suggesting possible PFO or a small ostium secundum ASD. In 3 goats this was only observed awake, in 4 only during general anesthesia, and in 2 during both examinations (Fig. 3B). Subsequently performed saline contrast studies did not indicate right-to-left shunting in any of the goats, neither awake nor during general anesthesia. However, in all but 2 goats (both in general anesthesia) undergoing a contrast study, a distinct negative contrast pattern

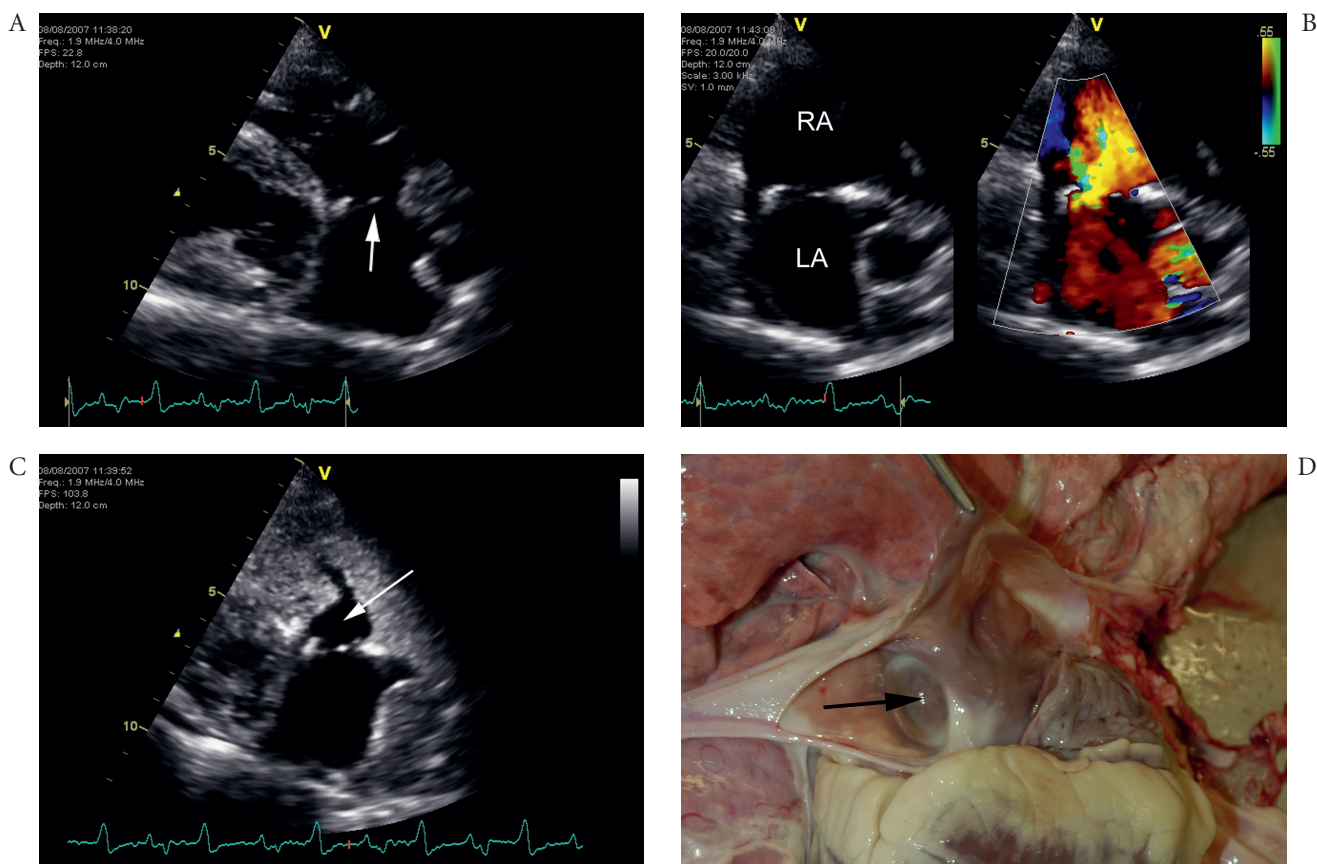


**Figure 3:** Echocardiographic recordings of a 6-year-old, 53 kg female Saanen goat, obtained in an awake, standing position. A, 2DE recording in a right parasternal long-axis view, focused on the interatrial septum. Part of the interatrial septum appears as a thin, echolucent membrane (arrow). B, Color Doppler imaging suggests systolic blood flow from the left (LA) into right (RA) atrium, crossing the interatrial septum. Turbulent flow is displayed in green. The corresponding 2DE image is displayed on the left. C, Saline contrast study showing marked saline contrast in the right atrium with a distinct negative contrast pattern adjacent to the interatrial septum (arrow). D, Opened right atrium on post mortem examination. The oval fossa (arrow) was clearly demarcated. Although the echocardiographic findings in this goat were suggestive of an interatrial communication with left-to-right shunting of blood, the atrial septum was completely developed and the foramen ovale was not patent.

560 Originalarbeiten

Table 3: Variables of left-ventricular dimensions and mechanical function using M-mode (MIME) and two-dimensional echocardiography (2DE).

Variable	Units	Awake			Anesthetized			Paired t-Test		
		n	Mean ± SD	5–95 % percentile	n	Mean ± SD	5–95 % percentile	95 % CI for difference of means	p-value	Significant after Bonferroni correction (P < 0.0014)
Left ventricle – MME short-axis view										
HR	min <sup>-1</sup>	21	93 ± 18	60–130	22	86 ± 11	70–110	-15.53 to 2.95	0.171	n.s.
IVS <sub>d</sub>	cm	21	1.1 ± 0.1	0.9–1.3	22	1.2 ± 0.2	0.9–1.7	-0.001 to 0.18	0.053	n.s.
IVS <sub>s</sub>	cm	21	1.4 ± 0.2	1.1–1.8	22	1.5 ± 0.2	1.2–1.9	-0.004 to 0.18	0.059	n.s.
LVID <sub>d</sub>	cm	21	4.4 ± 0.4	3.7–5.3	22	4.7 ± 0.8	3.9–7.1	0.15 to 0.64	0.003	n.s.
LVID <sub>s</sub> [60]	cm	21	4.4 ± 0.4	3.8–5.4	22	4.8 ± 0.8	3.6–7.2	0.15 to 0.66	0.003	n.s.
LVID <sub>d</sub> /AAD		21	1.77 ± 0.17	1.57–2.13	21	1.96 ± 0.29	1.58–2.86	0.07 to 0.31	0.004	n.s.
LVID <sub>s</sub>	cm	21	2.8 ± 0.4	2.1–3.5	22	2.7 ± 0.4	2.2–3.6	-0.25 to 0.06	0.200	n.s.
LVID <sub>d</sub> [60]	cm	21	2.8 ± 0.4	2.1–3.6	22	2.7 ± 0.5	2.1–3.7	-0.24 to 0.06	0.235	n.s.
LVID <sub>d</sub> /AAD		21	1.12 ± 0.12	0.85–1.30	21	1.10 ± 0.15	0.84–1.46	-0.09 to 0.04	0.497	n.s.
LVFW <sub>d</sub>	cm	21	1.0 ± 0.2	0.7–1.3	22	1.2 ± 0.2	0.9–1.6	0.05 to 0.24	0.005	n.s.
LVFW <sub>s</sub>	cm	21	1.6 ± 0.3	0.9–2.1	22	2.0 ± 0.2	1.5–2.4	0.27 to 0.56	< 0.001	*
FS	%	21	36.8 ± 4.7	26.8–48.4	22	43.5 ± 5.7	32.7–51.2	3.37 to 10.28	< 0.001	*
RWT <sub>d</sub>		21	0.48 ± 0.06	0.38–0.61	22	0.51 ± 0.11	0.26–0.72	-0.03 to 0.06	0.417	n.s.
RWT <sub>s</sub>		21	1.11 ± 0.17	0.89–1.59	22	1.36 ± 0.22	0.95–1.68	0.12 to 0.36	< 0.001	*
MWT <sub>d</sub>	cm	21	1.0 ± 0.1	0.8–1.2	22	1.2 ± 0.2	0.9–1.5	0.04 to 0.19	0.005	n.s.
MWT <sub>s</sub>	cm	21	1.5 ± 0.2	1.2–1.7	22	1.8 ± 0.2	1.4–2.0	0.17 to 0.34	< 0.001	*
LAD <sub>ms</sub> /LVID <sub>d</sub>		21	1.35 ± 0.13	1.16–1.63	22	1.35 ± 0.18	0.91–1.66	-0.10 to 0.07	0.741	n.s.
Left ventricle – 2DE long-axis view										
HR	min <sup>-1</sup>	22	96 ± 22	65–147	22	85 ± 11	67–108	-21.32 to -0.12	0.048	n.s.
LVI <sub>A</sub> <sub>d</sub>	cm <sup>2</sup>	22	28.0 ± 5.0	20.5–40.1	22	29.0 ± 4.2	23.3–36.7	-0.78 to 2.81	0.253	n.s.
LVI <sub>A</sub> <sub>d</sub> [60]	cm <sup>2</sup>	22	28.4 ± 5.9	20.3–42.0	22	29.3 ± 4.5	21.7–38.1	-0.88 to 2.68	0.304	n.s.
LVI <sub>A</sub> <sub>d</sub> /AAD <sup>2</sup>		22	4.66 ± 0.90	2.99–6.10	21	4.98 ± 0.91	3.49–6.38	-0.10 to 0.71	0.130	n.s.
LVI <sub>A</sub> <sub>s</sub>	cm <sup>2</sup>	22	10.9 ± 2.5	7.7–18.8	22	9.7 ± 2.5	6.0–15.1	-2.20 to -0.25	0.016	n.s.
LVI <sub>A</sub> <sub>s</sub> [60]	cm <sup>2</sup>	22	11.1 ± 2.9	6.6–19.7	22	9.8 ± 2.6	5.7–15.7	-2.27 to -0.31	0.012	n.s.
LVI <sub>A</sub> <sub>s</sub> /AAD <sup>2</sup>		22	1.81 ± 0.40	1.22–2.74	21	1.64 ± 0.42	1.08–2.59	-0.36 to -0.01	0.037	n.s.
FAC	%	22	61.1 ± 4.8	51.6–70.9	22	66.8 ± 5.6	58.4–77.5	3.02 to 8.24	< 0.001	*
LAA <sub>ms</sub> /LVI <sub>A</sub> <sub>d</sub>		22	0.79 ± 0.11	0.57–0.99	22	0.83 ± 0.11	0.66–1.09	-0.02 to 0.10	0.169	n.s.
LVI <sub>V</sub> <sub>d</sub>	mL	22	84.2 ± 22.4	53.5–143.0	22	91.1 ± 22.2	62.3–132.4	-0.45 to 14.12	0.065	n.s.



Table 3: (Continuation) Variables of left-ventricular dimensions and mechanical function using M-mode (MME) and two-dimensional echocardiography (2DE).

Variable	Awake		Anesthetized		Paired t-Test				
	n	Mean ± SD	5–95% percentile	n	Mean ± SD	5–95% percentile	95% CI for difference of means	p-value	Significant after Bonferroni correction (P < 0.0014)
HR	22	86.2 ± 26.1	46.1–153.2	22	92.6 ± 24.3	52.6–141.8	-0.57 to 13.29	0.070	n.s.
IVS <sub>i</sub>	22	20.0 ± 8.2	9.7–46.9	22	17.3 ± 6.8	8.6–32.3	-5.64 to 0.12	0.060	n.s.
IVS <sub>e</sub>	22	20.5 ± 9.1	7.7–50.2	22	17.59 ± 7.31	8.0–34.0	-5.87 to -0.01	0.049	n.s.
LVID <sub>d</sub>	22	1.34 ± 0.49	0.69–2.59	21	1.21 ± 0.48	0.69–2.42	-0.35 to 0.02	0.082	n.s.
LVID <sub>d</sub> /AAD <sup>s</sup>	22	76.3 ± 4.9	66.5–84.6	22	81.1 ± 4.2	74.4–88.8	2.44 to 7.23	< 0.001	*
EF	22	64.1 ± 16.2	39.7–98.0	22	73.7 ± 17.1	51.2–102.1	3.51 to 15.70	0.004	n.s.
SV	22	1.09 ± 0.32	0.61–1.75	22	1.25 ± 0.31	0.68–1.82	0.06 to 0.25	0.002	n.s.
SVI	22	6.0 ± 1.4	3.9–8.6	22	6.3 ± 1.8	3.5–9.1	-0.51 to 1.20	0.407	n.s.
CO	22	101.7 ± 28.3	61.2–146.6	22	106.9 ± 32.6	46.6–169.5	-9.73 to 20.08	0.478	n.s.
CI	22	101.7 ± 28.3	61.2–146.6	22	106.9 ± 32.6	46.6–169.5	-9.73 to 20.08	0.478	n.s.

HR	Heart rate								
IVS <sub>i</sub>	Interventricular septal thickness at end-diastole								
IVS <sub>e</sub>	Interventricular thickness at peak systole								
LVID <sub>d</sub>	Left-ventricular internal diameter at end-diastole								
LVID <sub>d</sub> /AAD	Left-ventricular internal diameter at end-diastole (normalized to a body weight of 60 kg)								
LVID <sub>d</sub>	Left-ventricular internal diameter at end-diastole indexed to aortic annular diameter								
LVID <sub>d</sub> /ADD	Left-ventricular internal diameter at peak systole (normalized to a body weight of 60 kg)								
LVID <sub>d</sub> /AAD <sup>s</sup>	Left-ventricular internal diameter at peak systole indexed to aortic annular diameter								
LFW <sub>s</sub>	Left-ventricular free wall thickness at end-diastole								
LFW <sub>s</sub>	Left-ventricular free wall thickness at peak systole								
FS	Left-ventricular fractional shortening								
RWT <sub>d</sub>	Relative wall thickness at end-diastole								
RWT <sub>s</sub>	Relative wall thickness at peak systole								
MWT <sub>d</sub>	Mean wall thickness at end-diastole								
MWT <sub>s</sub>	Mean wall thickness at peak systole								
LAD <sub>max</sub> /LVID <sub>d</sub>	Ratio of maximal left-atrial diameter-to-left-ventricular internal diameter at end-diastole								
LVI <sub>A<sub>d</sub></sub>	Left-ventricular internal area at end-diastole								
LVI <sub>A<sub>d</sub></sub> /AA <sub>d</sub> <sup>s</sup>	Left-ventricular internal area at end-diastole (normalized to a body weight of 60 kg)								
LVI <sub>A<sub>d</sub></sub> /AA <sub>d</sub> <sup>s</sup>	Left-ventricular internal area at end-diastole indexed to squared aortic annular diameter								
LVI <sub>A<sub>s</sub></sub>	Left-ventricular internal area at peak systole	LVI <sub>A<sub>s</sub></sub>							
LVI <sub>A<sub>s</sub></sub> /AVD <sup>s</sup>	Left-ventricular internal area at peak systole (normalized to a body weight of 60 kg)	LVI <sub>A<sub>s</sub></sub> /AVD <sup>s</sup>							
FAC	Left-ventricular fractional area change	FAC							
LAA <sub>max</sub> /LVI <sub>A<sub>d</sub></sub>	Ratio of maximal left-atrial area-to-left-ventricular internal area at end-diastole	LAA <sub>max</sub> /LVI <sub>A<sub>d</sub></sub>							
LVI <sub>V<sub>d</sub></sub>	Left-ventricular internal volume at end-diastole	LVI <sub>V<sub>d</sub></sub>							
LVI <sub>V<sub>d</sub></sub> /AA <sub>d</sub> <sup>s</sup>	Left-ventricular internal volume at end-diastole indexed to cubed aortic annular diameter	LVI <sub>V<sub>d</sub></sub> /AA <sub>d</sub> <sup>s</sup>							
LVI <sub>V<sub>s</sub></sub>	Left-ventricular internal volume at peak systole	LVI <sub>V<sub>s</sub></sub>							
LVI <sub>V<sub>s</sub></sub> /AA <sub>d</sub> <sup>s</sup>	Left-ventricular internal volume at peak systole (normalized to a body weight of 60 kg)	LVI <sub>V<sub>s</sub></sub> /AA <sub>d</sub> <sup>s</sup>							
EF	Left-ventricular ejection fraction	EF							
SV	Stroke volume	SV							
SVI	Stroke volume index	SVI							
CO	Cardiac output	CO							
CI	Cardiac index	CI							

## 562 Originalarbeiten

was seen in the right atrium, adjacent to the oval fossa (Fig. 3C).

Post mortem examination on 12 goats revealed structurally normal great vessels, myocardial structures, and heart valves. The Ductus arteriosus was completely obliterated and the interventricular septum was intact in all goats. The oval fossa was clearly demarcated in all goats and measured between  $1 \times 1$  and  $2 \times 3$  cm. In 8/12 goats, the atrial septum was intact and the foramen ovale was not patent, whereas in 4/12 goats the foramen ovale was shown to be patent by means of a small probe. However, the foramen was small and the primum and secundum septa appeared normally developed. Of the 9 goats in which the echocardiographic findings were suggestive of an interatrial shunt, 7 underwent post mortem examination; PFO was confirmed in 3 and it was ruled out in 4 of the goats. In 1 goat, PFO had not been suspected based on echocardiographic findings but was found on post mortem examination. Hence, based in these data, performance of echocardiography to diagnose PFO in apparently healthy goats was characterized by a sensitivity of 0.75 (95% confidence interval: 0.19–0.99), a specificity of 0.50 (0.16–0.84), a positive predictive value of 0.43 (0.10–0.82), and negative predictive value of 0.80 (0.28–1.00).

## Discussion

The present study demonstrates the applicability of transthoracic echocardiography in standing, unsedated goats and in goats under general anesthesia. It further provides data on reference intervals of a variety of echocardiographic indices obtained in healthy goats and on the influence of general anesthesia on cardiac size and function as determined by echocardiography.

Only few data are currently available on echocardiography in healthy adult goats, most likely because clinically recognized cardiovascular disease is rare in this species (Smith and Sherman, 2009). Nonetheless, the lack of normal echocardiographic data is somewhat surprising, considering the fact that goats commonly serve as animal models for human cardiovascular disease and are used for studies of atrial fibrillation, chronic heart failure, valve replacement, or use of total artificial hearts (Smith and Shermann, 2009).

The data reported here are in good agreement with previously reported echocardiographic indices of LV size and function in 8 Swedish domestic goats of similar age (3–8 years) and body weight ( $51 \pm 2$  kg) (Olsson et al., 2001), taking into consideration that the methods used for measurement of aortic size, LA dimensions, stroke volume, and cardiac output were different from the methods used in the present study.

In this study, we attempted to correct for differences in body weight by normalizing measurements of size of the great vessels and chamber dimensions to a «standard» body weight of 60 kg and by indexing measurements to

aortic annular diameter. The differences in normal intervals observed before and after normalizing to 60 kg standard weight turned out to be very small and were not considered clinically relevant. This may at least in part be explained by differences in body condition, which could have influenced body weight without significantly altering cardiac size in some animals. However, the study design did not allow further exploration of the influence of body condition, as body condition scoring was not performed consistently.

Aortic annular diameter is less dependent on body condition and can be used as an inherent reference of body size (Brown et al., 2003). Indexing measurements to aortic annular diameter might therefore be more useful than correcting for body weight in animals that are overweight or underweight. Furthermore, indexing to aortic annular diameter may also be used when accurate measurements of body weight are not available. However, possible alterations of aortic annular diameter due to cardiac disease need to be considered.

Several echocardiographic indices proved to be significantly influenced by general anesthesia when assessed individually. However, when correcting for the family-wise error rate, only variables describing systolic LV function were significantly influenced by general anesthesia. Specifically, anesthesia-induced alterations indicated an overall increase in systolic LV performance in goats under general anesthesia compared to standing, awake goats, which was represented by an increase in ejection phase indices (FS, FAC, EF) and more pronounced thickening of the myocardial wall at peak systole. Interestingly, cardiac output and cardiac index were not significantly affected by general anesthesia in this study. Although the reliability and accuracy of cardiac output measurements using 2DE in goats is unknown, a study in foals revealed that 2DE methods using a variety of geometrical models (including modified Simpson's method) were generally superior to Doppler-based cardiac output estimates (Giguère et al., 2005). Furthermore, the SVI found in this study during general anesthesia was in good agreement with results of a previous study on the cardiovascular effects of isoflurane in goats (Hikasa et al., 1998), indicating that the current estimates of SV and CO might be reasonably accurate.

Increased systolic LV performance during general anesthesia seems counterintuitive. Generally, volatile inhalation anesthetics cause dose-dependent changes in cardiovascular performance, often including direct myocardial depression and decrease in sympathoadrenal activity, leading to a decrease in cardiac output and arterial blood pressure (Steffey et al., 2007). Indeed, the preliminary results of a concomitant study on the use of 2D speckle tracking for assessment of systolic LV function in goats (Berli et al., 2009) indicate that general anesthesia causes depression of myocardial contractility (represented by a reduction of longitudinal, radial and circumferential segmental strain rate). However, the net effect of general anesthesia on systolic LV performance depends

on the interacting effects of altered preload, afterload, contractility, and heart rate caused by anesthetic drugs, fluid therapy, and mechanical ventilation. Therefore, the apparent increase in systolic LV performance and maintenance of cardiac output during general anesthesia in the present study could be related to alterations in loading conditions, which are able to overcome direct myocardial depression. However, this remains purely speculative, because the current study design did not allow assessing the various factors influencing cardiac performance.

Great attention needs to be concentrated on the atrial septum in goats. Thinning, billowing, or flailing of the atrial septum in the region of the oval fossa was a common finding in this study population, and it seems likely that this might be a general finding in goats. However, exaggerated mobility of the atrial septum and, in the extreme form, an atrial septal aneurysm is frequently associated with a PFO in people (Feigenbaum et al., 2005). In our opinion, this is of great relevance, since this common finding in goats can easily lead to an incorrect diagnosis of a PFO or an ASD, particularly in cases with suboptimal image quality. Color Doppler imaging can help identifying abnormal, usually bidirectional transseptal blood flow through a PFO or an ASD (Feigenbaum et al., 2005; Boon, 2011). However, physiologic blood flow entering the RA from the caudal vena cava and the LA from the pulmonary veins can easily be mistaken for transseptal flow on Color Doppler recordings, particularly if the color signals appear simultaneously adjacent to the oval fossa and if color gain is set too high or color bleeding artefacts appear. Also, flow acceleration and turbulence through the defect itself may not be seen, as pressure gradients are small and the velocity of shunting blood may not exceed the Nyquist limit (Boon, 2011). Saline contrast studies help confirm interatrial right-to-left shunting through a defect and should always follow Doppler interrogation in cases where PFO or ASD is suspected. However, left-to-right shunting is more difficult to detect using saline contrast, since blood flow from the caudal vena cava (which enters the RA right next to the oval fossa) frequently causes a distinct negative contrast pattern within the right atrium, mimicking left-to-right transseptal flow. This effect is caused by incomplete mixture and streaming of blood entering the RA from the cranial (containing bubbles) and the caudal (not containing bubbles) vena cava, respectively, and therefore has to be considered a normal finding.

In this study, echocardiography was not very accurate for diagnosis of a PFO. However, post mortem examination was only performed on a subset of the population, and the small sample size did not allow establishing test characteristics with high confidence. Furthermore, the oval foramina were small and the interatrial septum was found to be normally developed in all goats undergoing post mortem examination. These findings were therefore not considered clinically relevant and likely represented physiologic anatomical variations. In people, PFO is very common and occurs with a prevalence of 25 to 30% of all adults

(Feigenbaum et al., 2005), similar to the findings of this study, in which presence of a PFO was confirmed in 3/12 goats.

In conclusion, this study provides normal reference intervals for a variety of 2DE and MME indices in healthy adult goats. Furthermore, the results indicate that general anesthesia using isoflurane caused significant increases in echocardiographic indices of LV systolic performance. Finally, the data show that thinning, billowing, or flailing of the atrial septum in the region of the oval fossa is a common, most likely physiologic finding in adult goats. Although, presence of a small PFO was common in the study population, it was considered a physiologic variation. Echocardiographic diagnosis of small interatrial communications is difficult and misdiagnosis of PFOs or ASDs must be avoided. Further studies will be necessary to investigate reliability of echocardiographic measurements in adult goats and to describe the echocardiographic diagnosis of pathologic cardiac conditions in this species.

## References

- Acorda J.A., Ong R.A.F., Maligaya R.L.: Ultrasonographic features of the heart in Philippine native goats (*Capra hircus*). Philipp. J. Vet. Med. 2005,42:66–74.
- Amory H., Jakovljevic S., Lekeux P.: Quantitative M-mode and two-dimensional echocardiography in calves. Vet. Rec. 1991, 128: 25–31.
- Amory H., Lekeux P.: Effects of growth on functional and morphological echocardiographic variables in Friesian calves. Vet. Rec. 1991, 128: 349–354.
- Amory H., Kafidi N., Lekeux P.: Echocardiographic evaluation of cardiac morphologic and functional variables in double-muscling calves. Am. J. Vet. Res. 1992, 9: 1540–1547.
- Berli A.J., Jud R., Steininger K., Schwarzwald C.C.: The use of strain, strain rate, and displacement by 2D speckle tracking for assessment of systolic left ventricular function in goats: Applicability and influence of general anesthesia. In: Research abstracts of the 2009 ACVIM Forum, Montreal, Quebec, Canada. J. Vet. Intern. Med. 2009, 23: 751.
- Boon J. A.: Veterinary Echocardiography. 2<sup>nd</sup> Ed., Wiley-Blackwell, Ames, 2011, 610 p.
- Braun U., Schweizer T.: Bestimmung der Herzdimension beim Rind mit Hilfe der 2-D-Mode-Echokardiographie. Berl. Münch. Tierärztl. Wschr. 2001, 114: 46–50.
- Braun U., Schweizer T., Pusterla N.: Echocardiography of the normal bovine heart: technique and ultrasonographic appearance. Vet. Rec. 2001, 148: 47–51.
- Buczinski S.: Cardiovascular ultrasonography in cattle. Vet. Clin. Food Anim. 2009, 25: 611–632.
- Brown D.J., Rush J.E., MacGregor J., Ross J.N. Jr., Brewer B., Rand W.M.: M-mode echocardiographic ratio indices in normal dogs, cats, and horses: a novel quantitative method. J. Vet. Intern. Med. 2003, 17: 653–662.

**564 Originalarbeiten**

Cornell C.C., Kittleson M.D., Della Torre P., Haggstrom J., Lombard C.W., Pedersen H.D., Vollmar A., Wey A.: Allometric scaling of M-mode cardiac measurements in normal adult dogs. *J. Vet. Intern. Med.* 2004, 18: 311–321.

Feigenbaum H., Armstrong W.F., Ryan T.: Feigenbaum's Echocardiography. 6<sup>th</sup> Ed., Lippincott Williams & Wilkins, Philadelphia, 2005, 790p.

Giguère S., Bucki E., Adin D.B., Valverde A., Estrada A.H., Young L.: Cardiac output measurement by partial carbon dioxide rebreathing, 2-dimensional echocardiography, and lithium-dilution method in anesthetized neonatal foals. *J. Vet. Intern. Med.* 2005, 19: 737–743.

Hallowell G. D., Potter T. J., Bowen I. M.: Methods and normal values for echocardiography in adult dairy cattle. *J. Vet. Cardiol.* 2007, 9: 91–98.

Hikasa Y., Okuyama K., Kakuta T., Takase K., Ogasawara S.: Anesthetic potency and cardiopulmonary effects of sevoflurane in goats: comparison with isoflurane and halothane. *Can. J. Vet. Res.* 1998, 62: 299–306.

Irmer M.: Computertomographische Untersuchung des Abdomens bei 30 Ziegen. Dissertation, University of Zurich, Vetsuisse Faculty, 2010.

Jud R., Picek S., Makara M. A., Steining K., Hässig M., Bettschart-Wolfensberger R.: Comparison of racemic ketamine and S-ketamine as agents for the induction of anaesthesia in goats. *Vet. Anaesth. Analg.* 2010, 37: 511–518.

Lang R. M., Bierig M., Devereux R. B., Flachskampf F. A., Foster E., Pellikka P. A., Picard M. H., Roman M. J., Seward J., Shanewise J., Solomon S., Spencer K. T., St John Sutton M., Stewart W.: Recommendations for chamber quantification. *Eur. J. Echocardiogr.* 2006, 7: 79–108.

Makara M.: Computed tomography and cross-sectional anatomy of the head in the normal goat. Dissertation, University of Zurich, Vetsuisse Faculty, 2010.

Moses B. L., Ross J. N.: M-mode echocardiographic values in sheep. *Am. J. Vet. Res.* 1987, 48: 1313–1318.

Ohlerth S., Becker-Birck M., Augsburg H., Jud R., Makara M., Braun U.: Computed tomography measurements of thoracic structures in 26 clinically normal goats. *Res. Vet. Sci.* 2010, Epub ahead of print. doi:10.1016/j.rvsc.2010.10.019.

Olsson K., Hansson K., Hydbring E., Winblad von Walter L., Häggström J.: A serial study of heart function during pregnancy,

lactation and the dry period in dairy goats using echocardiography. *Exp. Physiol.* 2001, 86.1: 93–99.

Pipers F.S., Reef V., Hamlin R.L., Rings D.M.: Echocardiography in the bovine animal. *Bovine Practitioner* 1978,13:114–118.

Schefer K. D., Bitschnau C., Weishaupt M. A., Schwarzwald C. C.: Quantitative Analysis of Stress Echocardiograms in Healthy Horses with 2-Dimensional (2D) Echocardiography, Anatomical M-Mode, Tissue Doppler Imaging, and 2D Speckle Tracking. *J. Vet. Intern. Med.* 2010, 24: 918–931.

Schwarzwald C. C., Schober K. E., Bonagura J. D.: Methods and reliability of echocardiographic assessment of left atrial size and mechanical function in horses. *Am. J. Vet. Res.* 2007, 68: 735–747.

Smith M. C., Sherman D. M.: Cardiovascular system. In: *Goat medicine*. 2<sup>nd</sup> Ed., Wiley-Blackwell, Iowa, USA, 2009, 319–338.

Steffey E. P., Mama K. R.: Inhalation Anesthetics. In: *Veterinary Anesthesia and Analgesia*. Eds. W. J. Tranquilli, J. C. Thurmon, and K. A. Grimm, Lumb & Jones, 4th ed, Blackwell Publishing, Ames, Iowa, 2007, 355–393.

**Acknowledgments**

We would like to thank Prof. U. Braun for putting the goats at our disposal and the veterinarians and grooms of the Farm Animal Department for animal care and animal handling. Dr. Tony Glaus is acknowledged for his critical review of the manuscript.

**Corresponding author**

Colin C. Schwarzwald  
PD Dr. med. vet., PhD, Dipl. ACVIM & ECEIM  
Equine Department, Vetsuisse Faculty  
University of Zurich  
Winterthurerstrasse 260  
CH-8057 Zurich, Switzerland  
E-Mail: ccschwarzwald@vetclinics.uzh.ch

Received: 1 April 2011

Accepted: 6 May 2011